



1 Multitemporal glacier inventory revealing four decades of 2 glacier changes in the Ladakh region

3 Mohd Soheb¹, Alagappan Ramanathan¹, Anshuman Bhardwaj², Millie Coleman^{2,3}, Brice Rea²,
4 Matteo Spagnolo², Shaktiman Singh², Lydia Sam²

5 ¹ School of Environmental Sciences, Jawaharlal Nehru University, India.

6 ² School of Geosciences, University of Aberdeen, United Kingdom.

7 ³ School of Natural and Built Environment, Queen's University Belfast, United Kingdom.

8

9 *Correspondence to:* Mohd Soheb (sohaib.achaa@gmail.com)

10

11 **Abstract.** Glacier inventories, and changes therein, play an important role in understanding glacier dynamics and
12 water resources over larger regions. In this study, we present a Landsat-based multi-temporal inventory of glaciers in
13 four Upper Indus sub-basins and three internal drainage basins in the Ladakh region for the years 1977, 1994, 2009
14 and 2019. The study records data on 2257 glaciers (>0.5 km²) covering ~7923 ±212 km² equivalent to ~30% of the
15 glaciers and ~89% of the glacierised area within the region. Results show that the highest concentration of glaciers is
16 found in the higher elevation zones, between 5000 and 6000 m a.s.l, with most of them facing north. The area and
17 length of nearly all the glaciers (~97%) have decreased over the past 42 years, by 6.9% and 12% respectively.
18 However, heterogeneity in glacier change was observed across the basins. Glaciers in Shayok Basin experienced the
19 least deglaciation (~3.9%), whereas Leh (~23%) and Tsokar Basin (~26%) experienced the greatest deglaciation over
20 the 42 years (1977-2019). The major factors contributing to such differences were temperature, precipitation and size
21 of the glaciers, with most changes occurring as a result of a drier winters and warmer summers. During the observation
22 period, the region showed a statistically significant (at p<0.01) increasing trend in mean annual, JJAS and winter
23 temperatures.

24

25 1. Introduction:

26 Himalaya is the largest storehouse of snow and ice outside the Polar Regions. This large reserve of water plays a
27 crucial role in the hydro-economy of the region (Bolch, 2019; Frey et al., 2014; Maurer et al., 2019; Pritchard, 2019).
28 Any change to the cryosphere would have a direct impact on the hydrology, further influencing the communities
29 downstream whose livelihood and economy relies on and are supported by the major river systems e.g., the
30 Brahmaputra, Ganges and Indus, among others. Melt water from this region feeds millions of people including
31 megacities like Delhi, Dhaka, Karachi, Kolkata and Lahore (Azam et al., 2021; Immerzeel et al., 2010; Singh et al.,
32 2016). Recent studies have reported that Himalayan glaciers are retreating at an alarming rate (Azam et al., 2021;
33 Bolch, 2019; Käab et al., 2015; Maurer et al., 2019; Pritchard, 2019; Shean et al., 2020, among others) with glaciers



34 of the Western Himalayas showing less shrinkage than the glaciers of the central and eastern parts (Azam et al., 2021;
35 Shukla et al., 2020; Singh et al., 2016). Glaciers in the nearby Karakoram region display long-term irregular behaviour
36 with frequent glacier advances/surges and minimal shrinkage, which is yet to be fully understood (Azam et al., 2021;
37 Bhambri et al., 2013; Bolch et al., 2012; Kulkarni, 2010; Liu et al., 2006; Minora et al., 2013; Negi et al., 2021).
38 Glaciers of the Karakoram region experienced an increase in area post-2000, due to surge-type glaciers. In just the
39 upper Shayok valley, as many as 18 glaciers, occupying more than one-third of the glacierised area, showed surge-
40 type behaviour (Bhambri et al., 2011, 2013; Negi et al., 2021). However, not all regions have been analysed at the
41 same level of temporal and spatial detail. In particular, our knowledge of glacier dynamics and their response to
42 climate change is still incomplete in the cold-arid, high-altitude Ladakh region (~105,476 km²) comprising both, the
43 Himalayan and Karakoram ranges.

44 The advent of remote sensing technologies has permitted the mapping and measuring of various glacier attributes even
45 in the absence of sufficient in-situ observations (Bhardwaj et al., 2015). Glacierised area estimations have often relied
46 on global and regional glacier inventories such as the Randolph Glacier Inventory (RGI), Global Land Ice Monitoring
47 from Space (GLIMS), Geological Survey of India (GSI) inventory and Space Application Centre India (SAC)
48 inventory, among others. However, given the large scale of these inventories, automated techniques are often
49 employed to map and calculate glacier extent, with differing levels of success. Additionally, varying quality of satellite
50 imagery acquired from different time periods are sometimes necessitated in high mountain areas, such as Ladakh.
51 Together, these two factors can lead to over- or under-estimation of glacier areas leading to erroneous information on
52 temporal change. Moreover, there is no available multi-temporal glacier inventory for the region, which can inform
53 us on the changes in the natural frozen water reserves which have put the water security of this entire cold-arid region
54 under significant stress during recent years. The residents of Ladakh have witnessed a decrease in agricultural yields,
55 the main driver of economic development of the region, due to a decrease in water resources (Barrett & Bosak, 2018).
56 The water scarcity together with an increase in tourism footprint (four times more tourists (327,366) in 2018 than
57 2010, a number that is more than the entire population of Ladakh) has led to a shift in livelihood from agriculture to
58 other commercial activities (Müller et al., 2020), though even the latter relies heavily on water resources. In order to
59 cope with water scarcity, some people of Ladakh have developed new water management techniques, commonly
60 known as ‘ice reservoirs’ or ‘ice stupas’, to supplement agricultural activities (Nüsser, et al., 2019a,b).

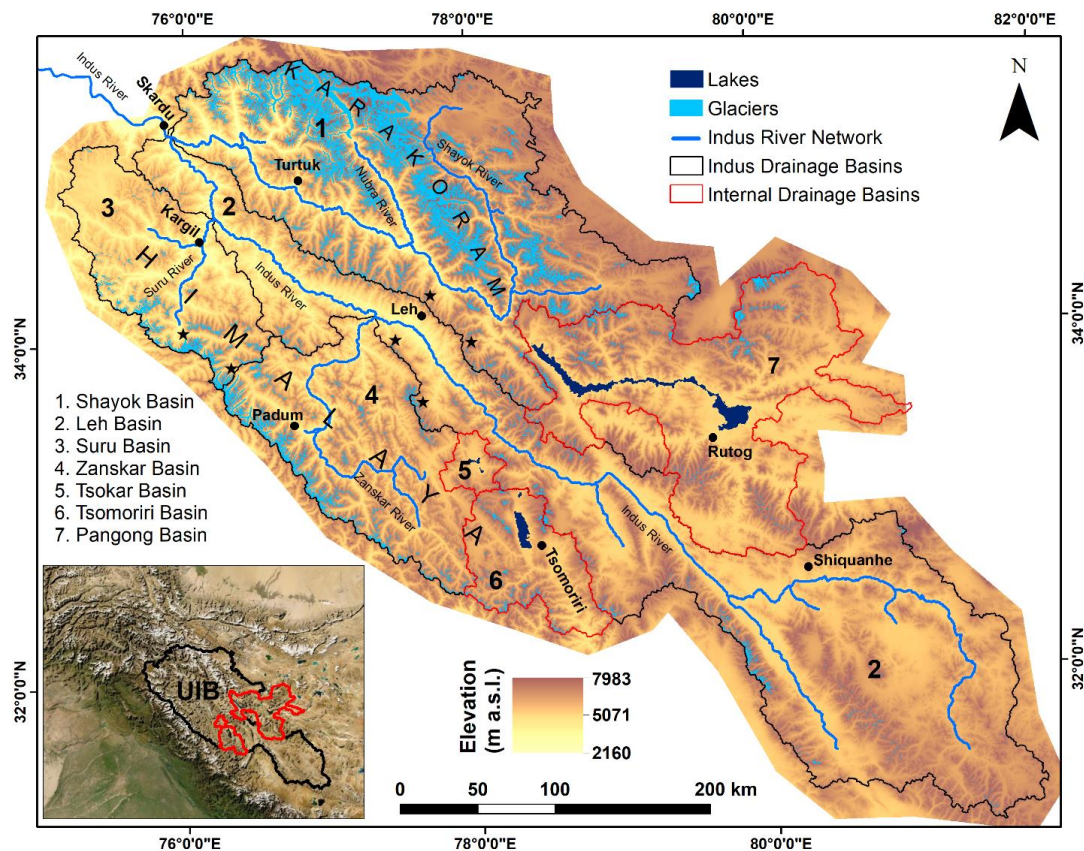
61 This study presents a new multi-temporal glacier inventory for the Union Territory of Ladakh, India, covering 42
62 years of change between 1977 and 2019. The inventories are entirely based on Landsat imageries acquired mostly
63 during late-summer with additional quality control provided through high-resolution PlanetScope and Google Earth
64 imagery. We further assess the rate of change of glaciers in response to the regional climate trends and other factors,
65 and establish a comparison with other inventories. This new dataset and analyses of glacier distribution and spatio-
66 temporal change will improve understanding of glacier dynamics and the impact of ongoing climate change on water
67 supplies in the Ladakh region, where water in the arid season is mostly supplied by glaciers. The dataset produced in
68 this study can be viewed here: <https://www.pangaea.de/tok/8b9a6e7275b32019eab155e11a461866706fabf3>
69 (temporary link for the reviewers’)

70



71
 72
 73

2. Study Area:



74

75 *Figure 1: Location map of the study area: the boundaries of studied Upper Indus Basin and internal drainage basins are outlined*
 76 *in black and red on the digital elevation model (DEM) and in the inset map. Inset map shows the study area with respect to the*
 77 *Himalayan and Karakoram region. Black dots and star represent the respective basins' major settlements and field investigated*
 78 *glaciers. ASTER Global DEM was used to produce the base map.*

79

80 This study focuses on glaciers in the Upper Indus Basin (Figure 1) upstream of Skardu (hereafter UIB) and three
 81 endorheic basins (or internal drainage basins, IDB hereafter) within the Ladakh region, namely Tsokar, Tsomoriri and
 82 Pangong basins. The geographic extent of the study area lies within a latitude of 31.1° to 35.6° N and a longitude of
 83 75.1° to 81.8° E and covers a vast region of the Karakoram and Western Himalayan ranges. UIB has an area of
 84 ~105,476 km², of which ~8302 km² (8%) is glacierised by ~6300 glaciers spanning elevations between ~3400 m and
 85 ~7500 m a.s.l. (as per RGI 6.0). IDBs of Tsokar (1036 km²), Tsomoriri (5462 km²) and Pangong (21,206 km²) house
 86 ~30, 345 and 812 glaciers, comprising a glacierised area of ~7 (0.6%), 185 (3.4%) and 437 (2.1%) km², respectively
 87 (as per RGI 6.0). The glaciers of IDBs are at a comparatively higher elevation, spanning from ~4800 to ~6800 m a.s.l.
 88 Meltwater from these glaciers drains into the lakes within each basin. Pangong Lake (a saline lake), situated at an



89 elevation of ~4250 m a.s.l., is the largest with an area of ~703 km². Both Tsomoriri (freshwater lake at ~4530 m a.s.l.)
90 and Tsokar (saline lake at ~4540 m a.s.l.) Lakes are designated Ramsar sites which occupy areas of ~140 and ~15
91 km², respectively.

92 Ladakh has a cold-arid climate due to the rain shadow and elevation effects of the Himalaya and Karakoram mountains
93 (Schmidt & Nüsser, 2017). Mean annual air temperature and annual precipitation range between -20 to 10 °C and 0 to
94 1800 mm, respectively (Hersbach et al., 2020). This region is inhabited by ~700,000 people (as per Census of India
95 2011, Census of China 2019), most of which are directly, or indirectly, dependent on snow and glacier meltwater to
96 support hydropower generation, irrigation and domestic needs.

97

98 **3. Data and methods**

99 **3.1. Data**

100 This study utilises multiple Landsat level-1 precision and terrain (L1TP) corrected scenes (63 scenes in total) from
101 four different periods: 1977±5 (hereafter 1977), 1994±1 (hereafter 1994), 2009 and 2019±1 (hereafter 2019). Scenes
102 from the 1970s are majorly (14 out of 17) from the year 1972 to 1977, however due to higher cloud cover and less
103 availability of imagery during the earlier Landsat period, three scenes from 1979 and 1980 were also included (Table
104 S1). Images from the late in the ablation season (July-October), having least snow and cloud cover (<30% overall,
105 and not over the glacierised parts), were selected and used for glacier identification and boundary delineation.
106 Advanced Space borne Thermal Emission and Reflection Radiometer Global Digital Elevation Model (ASTER DEM)
107 scenes were also used for basin delineation and calculating slope, aspect and elevation metrics of the glaciers. Glacier
108 digitisation, basin delineation and calculation of area were all performed in ArcGIS 10.4. Details of the imagery used
109 in this study are presented in (Table 1 and Table S1).

110 Additionally, long-term hourly ERA5 single level reanalysis temperature and precipitation data (Hersbach et al., 2020;
111 last accessed on 30 June 2020) have also been used to understand the regional climate and its evolution over the four-
112 decade window of interest. ERA5 is a fifth-generation ECMWF (European Centre for Medium-Range Weather
113 Forecasts) reanalysis dataset for global climate, at a high resolution (0.25°) and it has been shown to perform well for
114 the Ladakh region (Kanda et al., 2020). In-situ climate data from Leh (India, Indian Meteorological Department) and
115 Shiquanhe (China, <https://www.ncei.noaa.gov/>) were also used to bias correct the reanalysis dataset. Available time-
116 series datasets from the two stations (Leh and Shiquanhe) vary temporally. Leh station has around 27 years of data,
117 due to gaps ranging from months to years (Soheb et al., 2020) whereas, the Shiquanhe station comprises 38 years of
118 data for 1979 to 2019.

119

120

121

122



123 *Table 1: Information on the satellite imagery used in this study (Detailed info. in Table S1).*

Dataset	Year of Acquisition	Spatial Resolution	Source	Purpose
Landsat MSS	1977±5	60m	https://earthexplorer.usgs.gov/	Glacier area mapping
Landsat TM	1994±1, 2009	30m		
Landsat OLI	2019±1	15m		
ASTER GDEM	2000-2013	30m	https://earthdata.nasa.gov/	Topography and basin delineation

124

125

126 **3.2. Basin delineation**

127 Basin delineation was carried using ASTER GDEM V003 and the Hydrology tool in ArcGIS. The input DEM was
128 first analysed to fill-in all sinks with careful consideration of the potential for basin area over-estimation (Khan et al.,
129 2014). UIB was delineated using a pour point advertently selected at the Indus River in Skardu as we aimed to assess
130 all the tributary basins of the Ladakh region. The UIB obtained by this approach was further divided into second-order
131 tributary basins, i.e., Shayok, Suru, Zaskar and Leh basins. A small portion of the leftover area from UIB, after
132 second-order tributary basin delineation, was merged into the Leh basin so that the entire UIB, upstream of Skardu,
133 was investigated. Delineation of the three endoreic basins (IDBs) that lie partially or completely in the Ladakh region,
134 i.e., Tsokar, Tsomoriri and Pangong basins, was also carried out using the same method with the help of respective
135 lakes as a pour point.

136

137 **3.3. Glacier mapping**

138 Glaciers were mapped using a two-way approach, closely following the Global Land Ice Measurements from Space
139 (GLIMS) guidelines (Paul et al., 2009): 1) automatic mapping of the clean glacier and 2) manually correcting the
140 glacier outlines and digitisation of debris cover. First, a band ratio approach between NIR (Near Infrared) and SWIR
141 (Shortwave Infrared) (as suggested by Paul et al., 2002, 2015; Racoviteanu et al., 2009; Bhardwaj et al 2015; Schmidt
142 & Nüsser, 2017; Smith et al., 2015; Winsvold et al., 2014, 2016) with a threshold of 2.0 ($NIR/SWIR > 2 = ice/snow$)
143 was used on 2019 Landsat OLI images to delineate the clean part of glaciers. A median filter of kernel size 3 x 3 was
144 applied to remove the isolated and small pixels outside the glacier area. The NIR and SWIR band ratio approach is
145 good at distinguishing glacier pixels from water features with similar spectral reflectance values (Racoviteanu et al.,
146 2009; Zhang et al., 2019). This approach failed in areas with high snow/cloud cover, shadows, frozen channels/lakes
147 and debris cover. The snow/cloud cover and frozen lakes/stream problem were addressed by selecting Landsat scenes
148 from the ablation period (July-October) with the cloud cover < 30%. The issue with the snow-covered regions in
149 accumulation zones, where the delineation was the most challenging, was resolved using the best available imagery
150 of any time between 1977 and 2019 because glaciers are not expected to change their shape significantly in the higher
151 accumulation zones. One of the major issues was the debris covered glaciers, which had to be manually digitised, with
152 the support of high-resolution Google Earth and PlanetScope imagery from 2019 ±2. The result was then used as a
153 basis for manual digitisation of debris covered glaciers in other years where high-resolution images are not available.



154 In most cases, identification of the glacier terminus was made with certain contextual characteristics at the snout, e.g.,
155 the emergence of meltwater streams, proglacial lakes, ice walls, end moraines etc. (Figure S1).

156 The glacier outlines from 2019 were used as a starting point for the subsequent digitization of glacier areas of 2009,
157 1994 and 1977. Glacier length was measured using a semi-automatic approach, by employing the DEM to identify a
158 central flow line for each mapped glacier (Ji et al., 2017). Further manual corrections were undertaken to account for
159 the flow lines of glaciers that have multiple tributaries and multiple highest/lowest points. Furthermore, some mapping
160 errors are still expected to be present in this inventory due to a possible misinterpretation of glacier features, and the
161 quantification of such errors are difficult owing to the lack of reliable reference in-situ data in the Ladakh region. Such
162 errors were minimized by keeping a fixed map-scale of 1:10000 in most cases and doing a quality check on glacier
163 outlines using high-resolution images.

164 Other specific glacier attributes were also extracted including new glacier Ids, Global Land Ice Measurements from
165 Space (GLIMS)-Ids, Randolph Glacier Inventory (RGI 6.0)-Ids, coordinates (latitude and longitude), elevation
166 (maximum, mean and minimum), aspect (mean), slope (mean), area and length (maximum).

167

168 **3.4. Uncertainty**

169 The uncertainties associated with the glacier outline mapping originate from the spatial resolution of the satellite
170 images and the misleading effect of seasonal snow, shadow, debris and cloud cover. Due to the lack of ground truth
171 data for glaciers in the Ladakh region uncertainty estimation was performed following Paul et al., (2017). We applied
172 a buffer based assessment, with the buffer width set to one-pixel for debris and half-pixel for clean ice (Bolch et al.,
173 2010; Granshaw & G. Fountain, 2006; Mölg et al., 2018; Tielidze & Wheate, 2018), given that the level 1TP Landsat
174 images were corrected to sub-pixel geometric accuracy (Bhambri et al., 2013).

175 The associated uncertainty for smaller glaciers ($<0.5 \text{ km}^2$) amounts to ~15-30%, so all glaciers with an area of less
176 than 0.5 km^2 , which comprise ~70% and ~10% of the total glacier count and glacierised area, are not included in this
177 study. For the remaining glaciers, the uncertainty ranged between ± 2.7 and $\pm 10.3\%$ depending on the spatial resolution
178 of the satellite imagery and the individual glacier size. The highest uncertainty was for the year 1977 due to the coarser
179 spatial resolution of Landsat MSS data when applied to the smallest glaciers ($0.5\text{-}1 \text{ km}^2$). Overall, the uncertainty was
180 found to be 6% (Table S2).

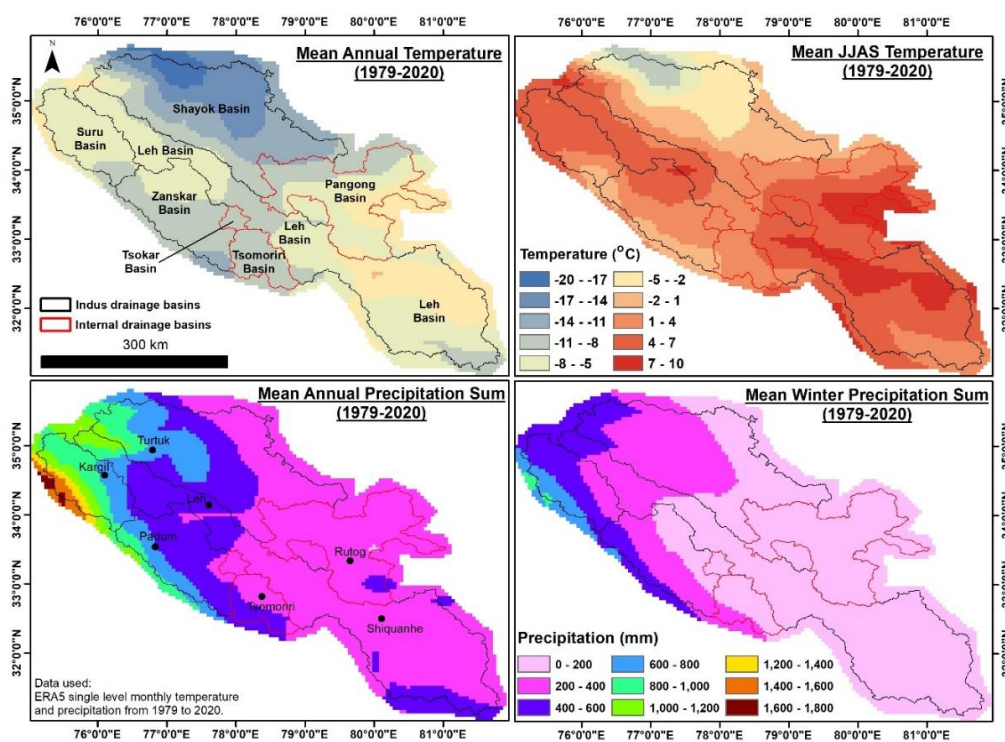
181

182 **3.5. Climate data correction and analysis:**

183 Kanda et al., 2020 evaluated the performance of seven gridded climate datasets (e.g., APHRODITE, CRU-TS, PGF,
184 UDEL, ERAI etc.) against observed data from the 19 in-situ stations scattered across the Karakoram, Greater and
185 Lower western Himalaya. It was found that ERA-Interim, with additional bias corrections, performed best. Since the
186 ERA5 is the improved version of ERA-Interim (Hersbach et al., 2020), it was further bias corrected and used to
187 understand the regional trends in temperature and precipitation, the first order driver of surface mass balance. Negi et
188 al., 2021 used 12 in-situ meteorological stations from the Shayok region and found the mean summer, mean winter



189 and mean annual temperature to be 3, -14 and -6.9 °C, respectively, between 1985 and 2015. The ERA5 reanalysis
190 data from the Shayok basin are in agreement with the in-situ temperatures.



191
192 *Figure 2: Distributive temperature (annual and JJAS) and precipitation (annual and winter) across the study area. Data used:*
193 *ERA5 single level monthly temperature and precipitation from 1979 to 2020, <https://climate.copernicus.eu/climate-reanalysis>*
194 The linear scaling bias correction method (Ines & Hansen, 2006; Shrestha et al., 2017; Teutschbein & Seibert, 2013)
195 was adopted for the corrections with the help of the available observed long-term Leh and Shiquanhe datasets. Only
196 seven grids from the entire region were bias corrected because of the limited observed dataset. One grid cell containing
197 a major village/town/city from each basin was chosen except for Tsokar and Leh basins. For the Leh basin two grid
198 cells were chosen because of the available observed records from Leh and Shiquanhe stations, whereas no grid cell
199 was chosen from the Tsokar basin due to its comparatively smaller area (Figure 1 and 2). The bias corrected data from
200 seven grids were further analysed statistically to understand the significance and magnitude of annual and seasonal
201 trends in temperature, precipitation and positive degree days (PDDs) using the Mann-Kendall test and Sen's slope
202 estimator (Sen, 1968), respectively. The change in temperature, precipitation and PDD was calculated following
203 Shukla et al., 2020.



204 **4. Results**

205 **4.1. Glacier inventory of 2019**

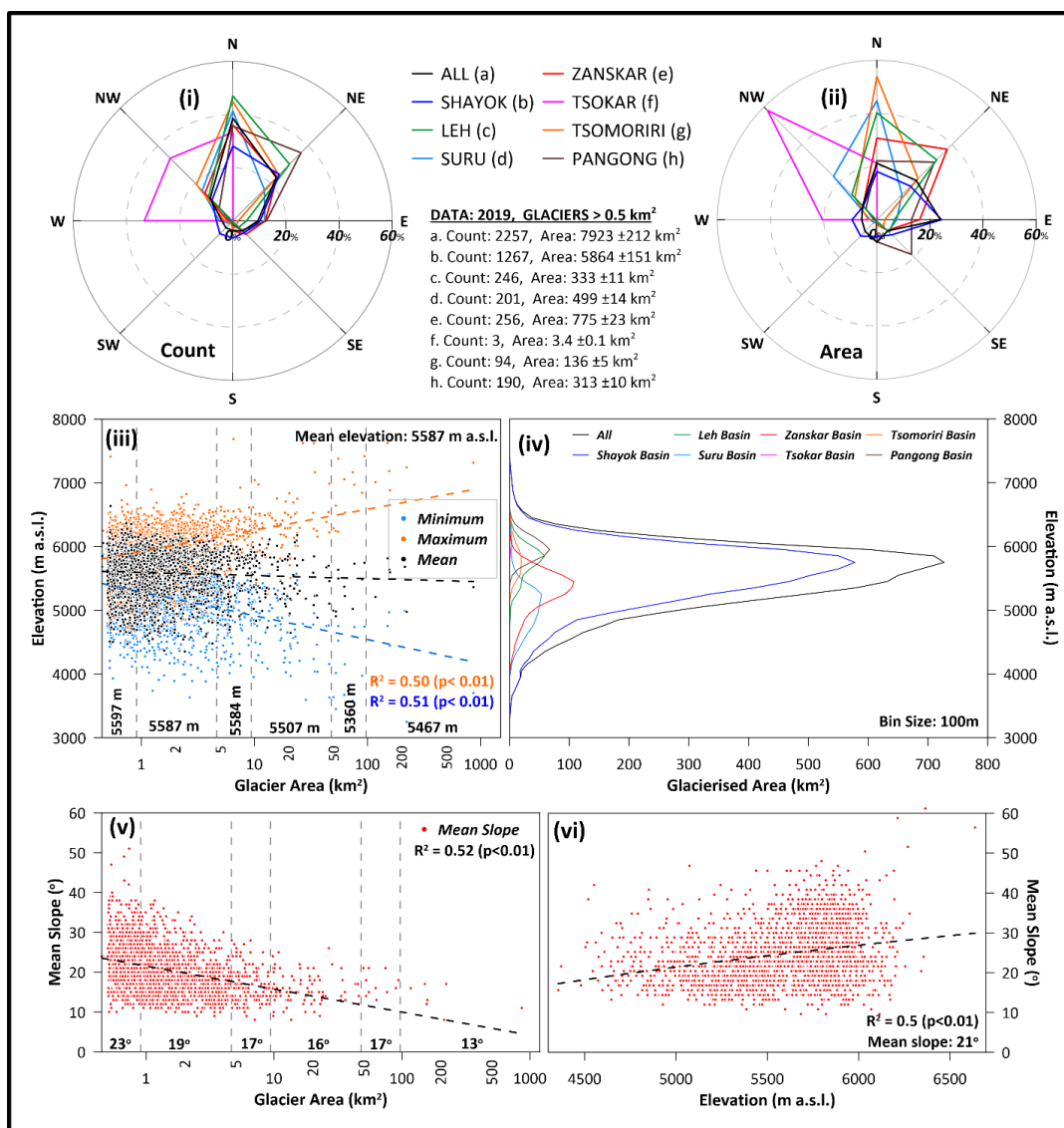
206 *Table 2: Basin-wide glacier information of UIB and IDBs based on present study for the year 2019.*

Basin	Basin area km ²	Total Area > 0.5 km ²		Area 0.5-1 km ²		Area 1-5 km ²		Area 5-10 km ²		Area 10-50 km ²		Area 50-100 km ²		Area > 100 km ²	
		Count	Area km ²	Count	Area km ²	Count	Area km ²	Count	Area km ²	Count	Area km ²	Count	Area km ²	Count	Area km ²
<i>All</i>	132180	2257	7923	980	694	1053	2206	124	853	84	1617	10	674	7	1879
<i>Shayok</i>	33579	1268	5864 (74%)	495 (51%)	351 (51%)	609 (58%)	130 (59%)	88 (71%)	621 (73%)	60 (71%)	115 (71%)	8 (80%)	559 (83%)	7 (100%)	1879 (100%)
<i>Leh</i>	46579	247 (11%)	334 (4%)	147 (15%)	105 (16%)	95 (9%)	191 (9%)	4 (3%)	26 (3%)	1 (1%)	12 (1%)	0	0	0	0
<i>Suru</i>	10502	201 (9%)	498 (6%)	81 (8%)	59 (9%)	100 (9%)	212 (10%)	12 (10%)	69 (8%)	8 (10%)	159 (10%)	0	0	0	0
<i>Zanskar</i>	14817	256 (12%)	775 (10%)	116 (12%)	82 (12%)	111 (11%)	235 (11%)	15 (12%)	108 (13%)	12 (14%)	235 (15%)	2 (20%)	115 (17%)	0	0
<i>Tsokar</i>	1036	3 (0.1%)	3.5 (0.04%)	2 (0.2%)	1.5 (0.2%)	1 (0.1%)	2 (0.1%)	0	0	0	0	0	0	0	0
<i>Tsomoriri</i>	5462	94 (4%)	135 (2%)	47 (5%)	22 (3%)	46 (4%)	95 (4%)	1 (1%)	7 (1%)	0	0	0	0	0	0
<i>Pangong</i>	21206	190 (8%)	315 (4%)	92 (9%)	63 (9%)	91 (9%)	168 (8%)	4 (3%)	22 (2%)	3 (4%)	60 (4%)	0	0	0	0

207



208



209

210 *Figure 3: General statistics of the glaciers in UIB and IDBs: orientation of glaciers (i) and associated area distribution (ii),*
 211 *Maximum, minimum and mean elevation of glaciers (iii), hypsometry of glacierised area (iv) and slope against glacier area (v)*
 212 *and elevation (vi).*

213

214 In 2019 the number of glaciers (>0.5 km²) is 2257 with an area totaling 7923 ± 212 km². The glacierised area amounts
 215 to ~6% of the overall region with glacier areas and lengths ranging between 0.5 to 862 km² and 0.4 to 73 km,
 216 respectively. Shayok Basin and glacier category of 1-5 km² occupies the highest glacierised area, whereas Tsokar
 217 Basin and glacier category of >100 km² comprise the least glacierised areas. Around 74% (1665) of the glaciers face

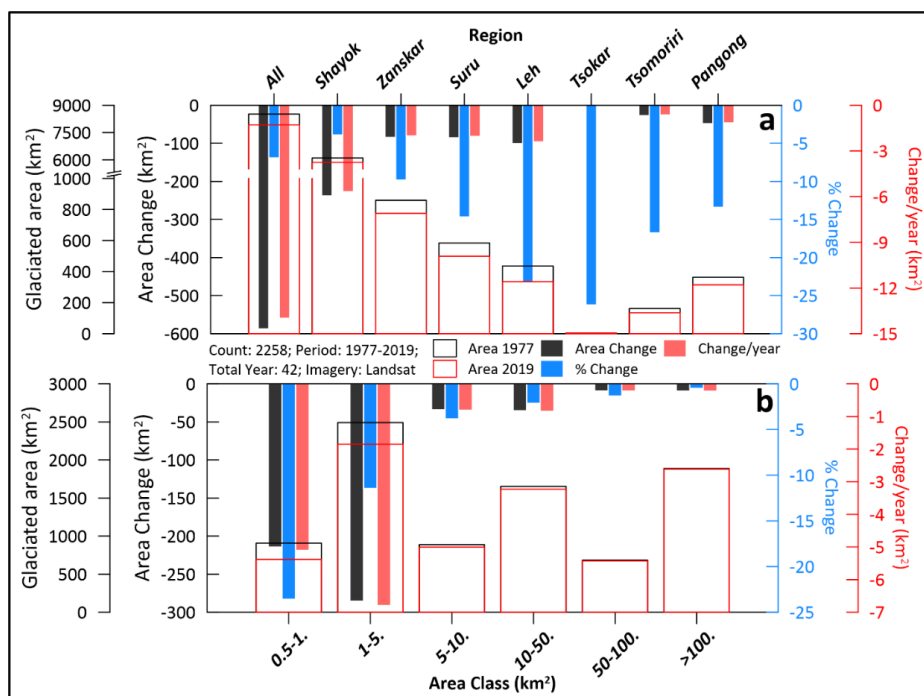


218 the northern quadrant (NW-N-NE) amounting to ~50% (3940 km²) of the glacierised area. However, the orientation
 219 and respective area coverage of glaciers varies within individual basins (Figure 3). Small glaciers were mainly found
 220 to occupy the higher elevations above 5500 and vice versa. The mean elevation of the glaciers for the entire study was
 221 ~5587 m a.s.l. and the majority (73%, 5810 km²) of the glacierised area is located between 5000 and 6000 m a.s.l.
 222 (Figure 3). The mean slope of these glaciers ranged between 8 and 46°, and was found to decrease with increasing
 223 glacier area. Glaciers with area greater than 100 km² have comparatively the lowest mean slope of 13° whereas, higher
 224 mean slopes (23°) were found for smaller glaciers. Overall, the mean glacier slope was ~21° (Figure 3).

225

226

4.2. Total glacier change between 1977 and 2019



227

228

Figure 4: Total change in the glacierised area with respect to a) basin and b) area class in 42 years (1977-2019).

229 The total glacierised area reduced from 8511 ±861 km² in 1977 to 7923 ±212 km² in 2019, revealing an overall change
 230 of ~-588 km² (-6.9%) in 42 years with a mean change of ~-14 km² year⁻¹ (-0.2% year⁻¹). The area change was found
 231 to be different for the individual UIB sub-basins and IDBs. Relative change in these basins ranged between -3.9 and
 232 -26%, with the least and greatest change found in Shayok and Tsokar basins, respectively (Figure 4). Glaciers in
 233 Shayok basin witnessed a change of ~-238 km² (~-5.7 km² year⁻¹) from 6102 ±595 km² in 1977 to 5864 ±151 km² in
 234 2019. Whereas, glacierised area of Tsokar basin reduced from 4.6 ±0.5 km² (1977) to 3.4 ±0.1 km² (2019), exhibiting
 235 a change of ~-1.2 km² (~-0.03 km² year⁻¹). Glacierised area in other basins also witnessed change ranging between ~-
 236 10 and -16% over 42 years.

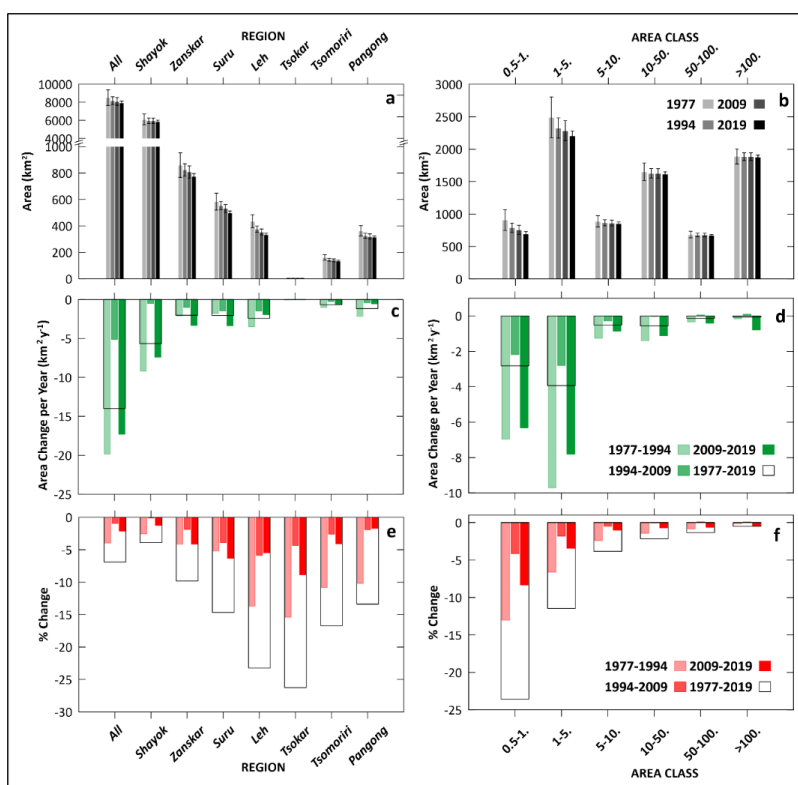


237 Deglaciation associated with different area classes ranged between -0.5 (>100 km²) to -24% ($0.5-1$ km²). Our results
 238 show that the highest relative change was mostly observed in the two smallest area classes of $0.5-1$ and $1-5$ km²
 239 whereas in larger area classes the change was found to be less than 4% . In the area category of $0.5-1$ km², where the
 240 maximum change happened, glacierised area reduced from 909 ± 161 km² (1977) to 694 ± 34 km² (2019), exhibiting a
 241 change of ~ -214 km² (-2.82 km² year⁻¹). The glaciers >100 km² witnessed a change of ~ -10 km² (-0.22 km² year⁻¹)
 242 from 1977 (1888 ± 115 km²) to 2019 (1879 ± 30 km²).

243

244

4.3. Periodical change in glacierised area between 1977 and 2019



245

246

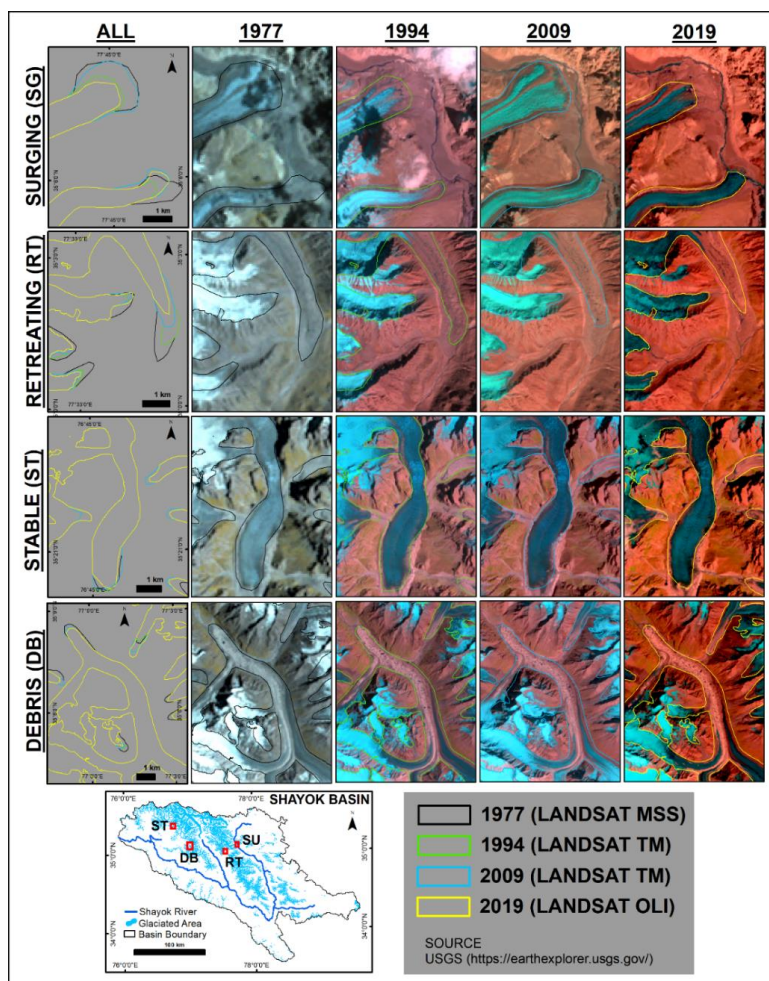
Figure 5: Periodical change in glacierised area: basin-wise (a, c, e) and area classes (b, d, f), between 1977 and 2019.

247

248 The results show that the deglaciation rate was variable across the measurement windows (1977-1994, 1994-2009 and
 249 2009-2019). The highest rate of change was found during the first period (1977-1994; -20 km² year⁻¹; -0.23% year⁻¹)
 250 followed by the third (2009-2019; -17 km² year⁻¹; -0.21% year⁻¹) whereas the second period (1994-2009) witnessed
 251 the lowest rate of change at ~ -5 km² year⁻¹ (-0.06% year⁻¹). A similar pattern of changes was found in most of the UIB
 252 sub-basins and in the three IDBs. But for the Zaskar and Suru basins, the rate of change was found to be highest in
 253 the third period (2009-2019) with -3.34 (-0.41% year⁻¹) and -3.37 km² year⁻¹ (-0.63% year⁻¹), respectively (Figure 5).



254 The maximum rate of change was found in the glaciers of 1-5 km², ~-10, -3 and -8 km² year⁻¹, equivalent to -0.77, -
 255 0.28 and -0.83% year⁻¹ during 1977-1994, 1994-2009 and 2009-2019, respectively. The lowest rate of change was
 256 observed in the larger, >100 km², glaciers with a change of -0.2 (-0.01% year⁻¹), +0.1 (+0.01% year⁻¹) and -0.8 (-
 257 0.04% year⁻¹) km² year⁻¹ during first, second and third periods. The period 1977-1994 witnessed the maximum
 258 deglaciation per year in all area classes except the two largest classes where maximum deglaciation happened during
 259 the third period (2009-2019). The lowest rate of change was observed during the second period (1994-2009) where
 260 the two largest area classes (50-100 and >100 km²) experienced a positive mean change of +0.05 and +0.1 km² year⁻¹
 261 equivalent to ~+0.01 and +0.01% year⁻¹, respectively. Some examples from the Shayok Basin of different type of
 262 glacier change i.e., surging, retreating, stable and change in high debris covered glacier are presented in Figure 6.



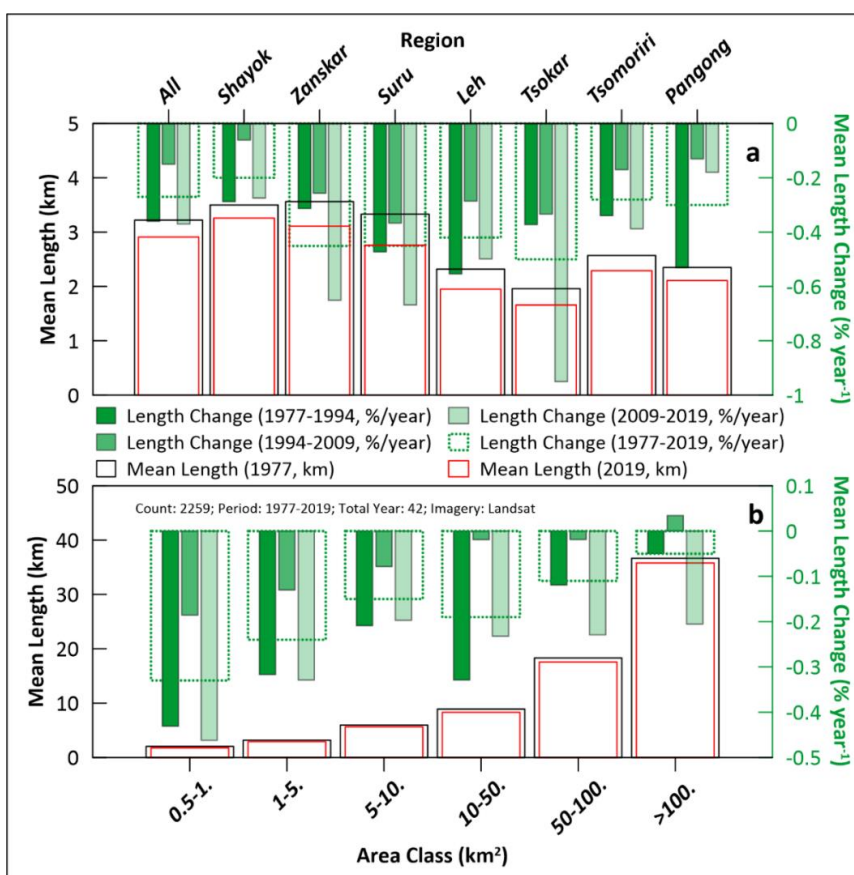
263
 264 *Figure 6: Examples of different types of glacier change from the Shayok basin: surging type, retreating, stable and high debris*
 265 *covered glacier between 1977 and 2019.*

266



267

4.4. Glacier length change between 1977 and 2019.



268

269

270

Figure 7: Temporal rate of change of glacier length in study area, basins and area classes.

271 Glacier lengths between 1977 and 2019 show a change ranging between +13 to -59% with the majority of retreat in
 272 the range of ~-5 to -30%. It was found that nearly all (97%) glaciers retreated over the measurement window with a
 273 mean retreat of ~-12% (-0.27% year⁻¹). Tsokar, Suru and Leh basin witnessed a comparatively higher rate of change
 274 ~-19, -19 and -18% equivalent to -0.5, -0.5 and -0.4 % year⁻¹, respectively. Whereas, change was relatively lower in
 275 Shayok (-8%), Zanskar (-15%), Tsomoriri (-12%), Pangong (-12%) and Shayok (-8%) from 1977 to 2019. For the
 276 area categories, the total length change ranges between -2.5 to -14% with the highest change found for the smallest
 277 area class (0.5-1 km²) and vice versa.

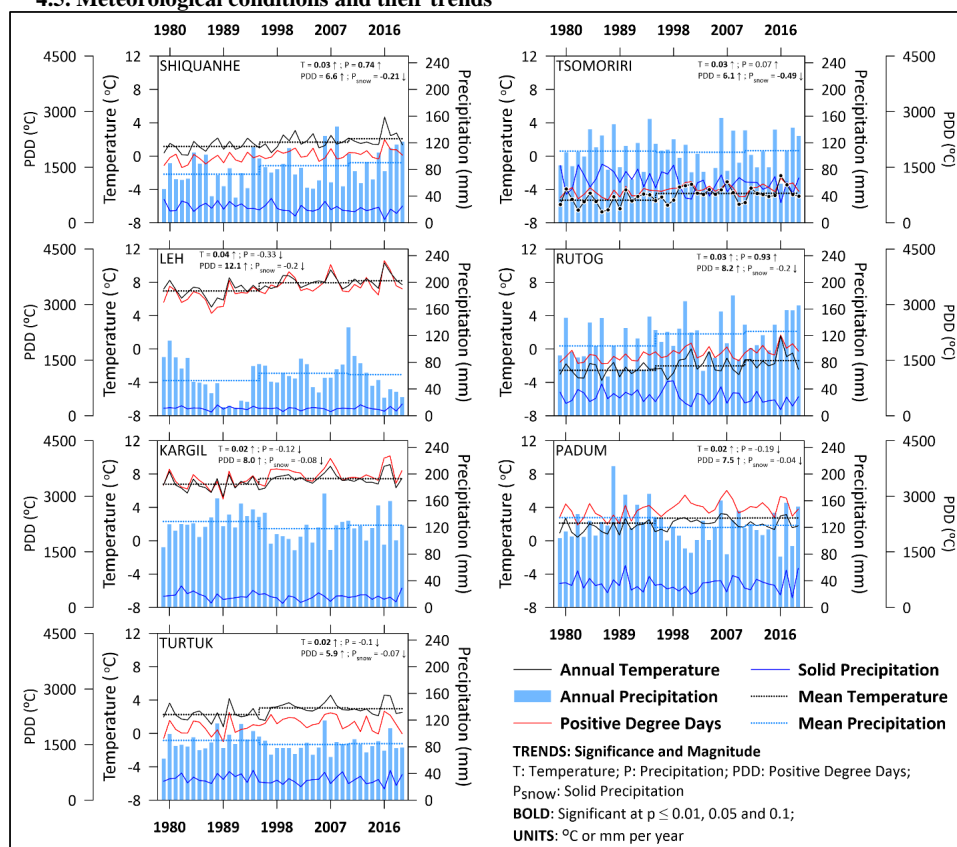
278 The mean rate of change in glacier length was temporally variable, -0.4, -0.2 and -0.4% year⁻¹ for 1977-1994, 1994-
 279 2009 and 2009-2019, respectively. The retreat rate for 1977-1994 was highest in Shayok, Leh and Pangong basins,
 280 and in the two area classes (5-10 and 10-50 km²). Other basins and area classes witnessed the highest rate in length



281 change during the period 2009-2019. The rate was found to be lowest during 1994-2009 in all basins and area classes
 282 (Figure 7) and a positive change was also observed in the largest area class, >100 km², during 1994-2009 as a result
 283 of glacier surging.

284
 285

4.5. Meteorological conditions and their trends



286

287 *Figure 8: ERA5 bias-corrected annual temperature (mean) and precipitation (sum) of the seven grids of the study area. Mean*
 288 *temperature (dotted line) represent mean of the period and PDD is the sum of degrees above 0 °C per day of the year.*

289

290 Meteorological conditions at the seven major settlements (Shiquanhe, Rutog, Leh, Turtuk, Tsomoriri, Padum and
 291 Kargil) are presented in Figure 8 and Figure S3. Figure S2 presents the correlation between observed and bias-
 292 corrected ERA5 reanalysis data. The result shows a strong correlation for temperature with $R^2 = 0.97$ ($p < 0.01$) at both
 293 Leh and Shiquanhe. A weaker but significant correlation was found for the precipitation at Shiquanhe ($R^2 = 0.54$, $p <$
 294 0.01) and Leh ($R^2 = 0.1$, $p < 0.01$). The mean annual temperature and total annual precipitation in the study area,
 295 during the 40-year period (1979-2019), ranged between -7 (Tsomoriri, 1986) to +10 °C (Leh, 2016) and 13 (Leh,
 296 1991) to 213 mm (Padum, 1988), respectively. The results show Leh and Kargil were comparatively the warmest,
 297 with annual PDD sums exceeding 3000 °C while Tsomoriri was the coldest where the annual PDD sum never exceeds



298 1500 °C. Kargil, Padum, Tsomoriri and Rutog were wetter than other major settlements with Leh being driest (Figure
299 2 and 8). Solid precipitation, which mostly falls during winter months, was <80 mm in all the locations with highest
300 found in Tsomoriri (40 to 80 mm). Leh, Kargil and Shiquanhe had the lowest (< 40 mm) annual solid precipitation
301 (Figure 8).

302 Between 1979 and 2019 all locations showed a statistically significant increasing trend in mean annual, JJAS and
303 winter air temperatures with Leh exhibiting the highest rate of increase in mean annual, JJAS and winter temperatures
304 (Figure 8, Table S3). Padum had the lowest increase in temperature. Statistically significant trends in precipitation
305 were observed only in Shiquanhe (annual, JJAS), Rutog (annual, JJAS) and Tsomoriri (winter). Shiquanhe and Rutog
306 had positive trend in annual and JJAS precipitation and Tsomoriri had a negative trend in winter precipitation and
307 Tsomoriri and Shiquanhe experienced a decrease in solid precipitation (Figure 8, Table S3). A statistically significant
308 increasing trend in annual PDD sums was observed in all locations ranging between 5.9 and 12.1 °C year⁻¹, (Figure 8,
309 Table S3).

310

311 5. Discussion

312 5.1. Description of the produced dataset and limitations

313 The entire dataset of the multitemporal inventories of glaciers (>0.5 km²) in Ladakh region for the year 1977, 1994,
314 2009 and 2019 is available at PANGAEA portal (<https://doi.org/10.1594/PANGAEA.940994>; Soheb et al., 2022).
315 The dataset are provided in two different GIS-ready file formats, i.e., GeoPackages (*.gpkg) and Shapefiles (*.dbf,
316 *.prj, *.sbn, *.sbx, *.shp, *.shx) to support a wider end users. GeoPackage is a relatively new and open file format
317 which is now being widely used and supported, whereas Shapefile format is one of the most widely used proprietary
318 but open file formats for vector datasets, supported by open-source GIS tools such as QGIS. The provided outlines of
319 glaciers, basins and lakes are all referenced to the WGS 84 / UTM zone 43N datum. For each region, there is one file
320 for basin and lake (if any) outlines, and four files for glacier outlines of 1977, 1994, 2009 and 2019. Each glacier
321 outline file contains glacier Ids (Jawaharlal Nehru University and University of Aberdeen glacier Ids, Randolph
322 Glacier Inventory 6.0 Ids, and Global Land Ice Measurements from Space initiative Ids), coordinates (latitude and
323 longitude), elevation (maximum, mean and minimum), aspect (mean), slope (mean), area and length (maximum).
324 While using this dataset, it is important to understand the key limitations of such regional-scale glacier inventories.
325 Some of the key user limitations of the produced dataset are: (1) Glaciers smaller than 0.5 km² (which comprise ~70%
326 and ~10% of the total glacier population and glacierised area, respectively) were not included in this inventory due to
327 the higher uncertainty (~15-30%) associated with these glacier outlines; (2) Inventories produced in this study are
328 entirely based on the medium resolution Landsat imageries, in the same way as other global or regional-scale glacier
329 inventories. Although the uncertainty associated with these inventories do not considerably impact regional-scale
330 analyses, care should be taken while using this data for a small set of glaciers. It should also be noted that it is not
331 feasible to produce multitemporal inventories regionally using high-resolution datasets due to scarce availability and
332 high costs of such high-resolution datasets; (3) The inventories of 1977±5, 1994±1 and 2019±1 are produced using
333 images with a range of acquisition dates due to the lack of data continuity within a particular year (more details in



334 section 3.1); and (4) The time periods chosen in this study are based on the availability of datasets and sufficient
335 temporal gaps among the datasets to allow multi-temporal glacio-hydrological analyses for a user.
336

337 **5.2. Significance of the present inventory**

338 The glacier inventory presented here has several improvements compared to the existing regional and global
339 inventories. Firstly, it covers the glaciers ($> 0.5 \text{ km}^2$; $n = 2257$; $\sim 7923 \pm 212 \text{ km}^2$) for the entire Ladakh region with
340 manual correction and quality control undertaken using freely available high-resolution images. The analyses were
341 further extended to estimate the change and distribution of ice masses at sub-basin scale. Secondly, for all the glaciers
342 a temporal rate of change has been calculated, which will aid hydrological and glaciological modelling aimed at
343 understanding past and future evolution. Finally, the new inventory will aid both the scientific community studying
344 the glaciers and water resources of the Ladakh region, and the administration of the Union Territory of Ladakh,
345 Government of India in developing efficient mitigation and adaptation strategies by improving the projections of
346 change on timescales relevant to policy makers.

347 **5.2. Glacier and climate of the region**

348 Overall, the majority (97%) of the glaciers in the Ladakh region retreated over the study period. The results,
349 unsurprisingly, also show a considerable heterogeneity. The Shayok Basin glaciers experienced the least change while
350 the Leh Basin deglaciated most. Some of the major factors contributing to such contrasting changes within this
351 region include climate (temperature and precipitation), topography, elevation, orientation, and glacier size. Most
352 documented changes appear to be occurring as a result of increasingly drier and warmer summers (lower precipitation
353 due to a weakened Indian Summer Monsoon) and wetter winters (particularly snow due to Western Disturbances)
354 (Farinotti et al., 2020; Yao et al., 2012). The moisture-laden ISM and WD (during summer and winter, respectively)
355 deliver precipitation mostly on the major orographic barriers of the Greater Himalayan and the Karakoram ranges, but
356 only limited precipitation bearing air masses reach the Ladakh region, specifically Leh and Tsokar basins resulting in
357 a greater deglaciation. However, glaciers of Suru, Zaskar, Tsomoriri and Pangong basins, which are proximal to the
358 major orographic barriers (Greater Himalayan and Karakoram ranges), showed comparatively moderate retreat.

359 The predominance of small glaciers in the Leh (97%), Tsokar (100%) and Tsomoriri (98%) basins is also a reason for
360 the contrasting behavior in glacier change. The smaller glaciers displayed the greatest deglaciation as they are more
361 sensitive to changes in surface mass balance (Yang et al., 2020). A small increase in ELA or SLA can turn these small
362 glaciers entirely into ablation zone, thus negatively impacting their health. Results also show that smaller glaciers
363 generally have steeper slopes thus experiencing a larger relative area loss than less steep glaciers.

364

365 **5.3. Comparison of inventories in the Ladakh region**

366 *Table 3: Basin and class wise comparison of the glacierised area between the present study and other inventories (RGI 6.0,*
367 *ICIMOD and GAMDAM).*

Region	Present Study	RGI 6.0	GAMDAM	ICIMOD
--------	---------------	---------	--------	--------

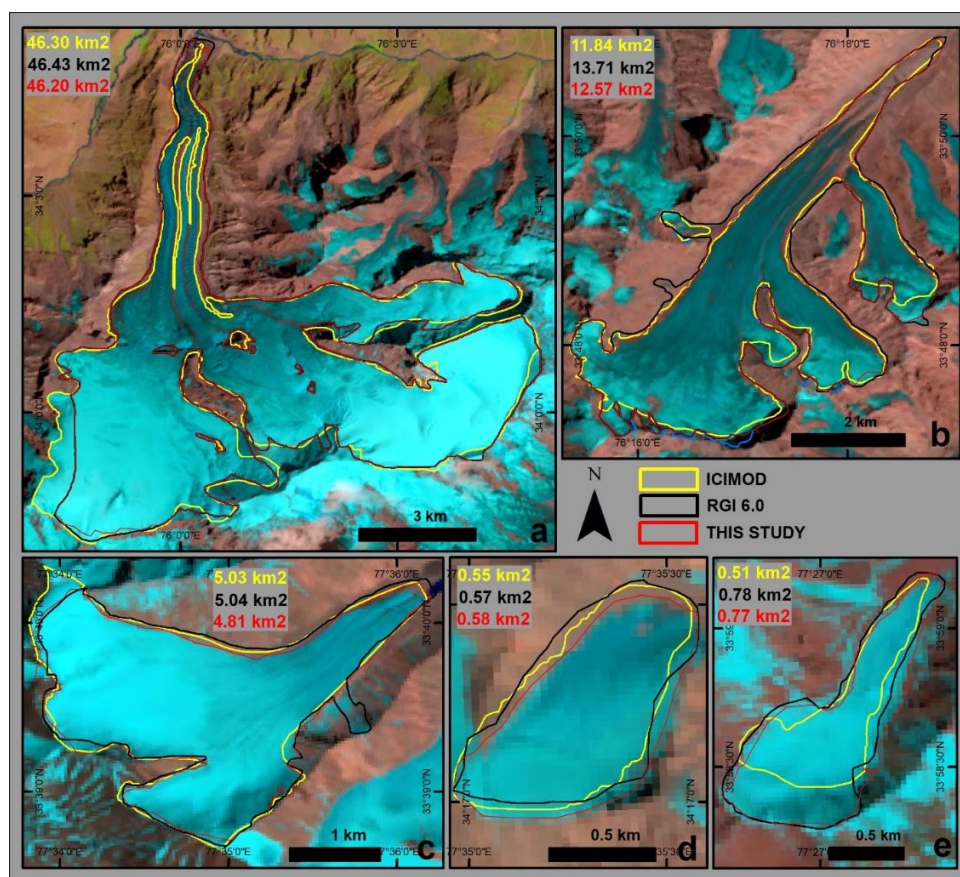


	Area	Area	Difference		Area	Difference		Area	Difference	
	km ²	km ²	km ²	%	km ²	km ²	%	km ²	km ²	%
Shayok	5938	6999	1061	15	6616	678	10	5456	-482	-9
Zanskar	808	880	72	8	932	124	13	819	11	1
Suru	532	525	-7	-1	564	32	6	506	-26	-5
Leh	354	342	-12	-3	356	2	1	322	-32	-10
Tsokar	4	4.4	1	15	4.3	1	13	4.1	0	9
Tsomoriri	141	142	1	1	143	2	2	116	-25	-21
Pangong	320	320	0	0	335	15	4	-	-	-
Area Class										
0.5-1	758	774	16	2	803	45	6	662	-96	-7
1-5.	2284	2437	153	6	2385	101	4	1958	-326	-12
5-10.	862	961	99	10	925	63	7	766	-96	-10
10-50.	1628	1959	331	17	1824	196	11	1356	-272	-20
50-100	678	730	52	7	599	-79	-13	592	-86	-15
>100	1887	2351	464	20	2412	525	22	1887	0	0
Total	8096	9212	1116	14	8950	854	11	7223	-533	-7

368

369 Differences in estimates of the glacierised areas are meaningful as they can lead to an over or under estimation of the
 370 available water resources. Therefore, correctly estimating glacier change over time is necessary for understanding
 371 glacier dynamics, future response to climate forcing and the water resources they provide. Table 3 presents a
 372 comparison between the present inventory and the Randolph Glacier Inventory (RGI) 6.0 (Pfeffer et al., 2014),
 373 International Centre for Integrated Mountain Development (ICIMOD) inventory (Bajracharya et al., 2019; Williams,
 374 2013) and Glacier Area Mapping for Discharge in Asian Mountains (GAMDAM) inventory (Guo et al., 2015; Sakai,
 375 2019), for the Ladakh region. The comparison involves glacier outlines for 2009 from the present study and excludes
 376 glaciers smaller than 0.5 km² from regional inventories to achieve the closest match temporally and for glacier size
 377 categories. Figure 9 presents a comparison of the only three inventories (present, RGI 6.0 and ICIMOD) on the five
 378 field-investigated glaciers of Ladakh region because RGI and GAMDAM inventory share the same outlines on these
 379 glaciers.

380 The comparison showed a higher glacierised area in RGI and GAMDAM inventories and lower in the ICIMOD
 381 inventory (Table 3) than the present inventory, with most of the differences contributed by the basins having the higher
 382 glacierised areas (Shayok and Zanskar) and from the larger glaciers (>10 km²). Such inconsistencies among the
 383 inventories are a product of several factors, e.g. 1) absence of change in glaciers over time due to the use of imagery
 384 with a wide range of acquisition years (Figure 9 a, c, d); 2) misinterpretation of the glacier terminus due to icing,
 385 debris, snow and cloud cover (Nagai et al., 2016), and 3) the methodology used. The smaller difference between the
 386 present and the ICIMOD inventory is mainly due to the adoption of a similar technique (i.e., a semi-automated
 387 approach) and the shorter time frame of the analysis that generated the ICIMOD inventory (i.e., 2002-2009).



388

389 *Figure 9: Comparison of inventories on the field investigated glaciers of the study area: a) Parkachik glacier, Suru Basin; b)*
 390 *Pensila glacier, Suru Basin; c) Lato glacier, Leh Basin; d) Khardung glacier, Shayok Basin; e) Stok glacier, Leh Basin.*

391

392 5.4. Comparison with recent studies

393

Table 4: Comparison of glacier change attributes between the present study and others recent studies.

Region	Study	Period	Total Glaciers	Glacier Size (km ²)	Area Change (km ²)	Area Change (%)	Area Change /year (%)
Shayok Basin	Present	1994-2009	1267	>0.5	-7.56	-0.12	-0.008
		1994-2019	1267	>0.5	-81.69	-1.4	-0.05
	Negi et al., 2021*	1991-2014	569	>1	-7.8	-0.91	-0.008
Leh Basin	Present	1977-2019	247	>0.5	-102	-23	-0.5
	Schmidt and Nüsser, 2017*	1969-2016	135	>0.03	-21.79	-19	-0.4
Suru Basin	Present	1977-2019	201	>0.5	-85.78	-14	-0.3
	Shukla et al., 2020*	1971-2017	240	>0.01	-32	-6	-0.2

394

395

396

**Negi et al., 2021 basin area is comparatively small and within Indian territory only; *Schmidt and Nüsser, 2017 studied temporal changes in few selected glaciers; *Shukla et al., 2020 studied the Suru sub-basin only.*



397 For the glaciers of the Shayok Basin our results agree with Negi et al., 2021, showing similar retreat rates (Table 4)
398 and lower summer, winter and annual temperatures reported over similar periods 1979-2019 (this study) versus 1985-
399 2015 (Negi et al., 2021). The lower summer temperatures and higher precipitation provide one explanation for the
400 area having the least change, apart from the 'Karakoram Anomaly', which is still not completely understood (Azam et
401 al., 2018, 2021; Bhambri et al., 2013; Hewitt, 2005; Minora et al., 2016; Negi et al., 2021). Another contributing factor
402 is likely due to higher proportion of surge-type glaciers which occupy a larger proportion of the glacierised area in the
403 Karakoram (Bhambri et al., 2013, 2017). Greater retreat in the glaciers in the Leh Basin (higher than the western
404 Himalayan average retreat rate of ~ 4 % year⁻¹, Shukla et al., 2020) appears to be driven by comparatively higher JJAS
405 temperatures and lower winter precipitation (Figure 2, 8). Leh Basin is narrow and long (~ 700 km) with relatively
406 high mean air temperature (both mean annual and JJAS) and low precipitation (total annual and winter precipitation)
407 in the region, especially in the area (Figure 2) where majority ($\sim 80\%$) of the glaciers are located. Retreat rates for
408 glaciers in the Leh basin from Chudley et al., 2017; Schmidt & Nüsser, 2012, 2017 and this study are all in agreement
409 (Table 4).

410 The relatively moderate retreat in the Suru and Zaskar Basins (Figure 4, 5, 7) is the result of a higher population of
411 large glaciers and meteorological conditions, particularly higher JJAS temperature and higher winter precipitation
412 (Figure 8) which appear to have somewhat cancelled each other out. Zaskar and Suru Basin results are also in line
413 with the recent finding by Maurer et al., 2019 and Shukla et al., 2020 which observed that the average mass loss had
414 doubled post-2000 i.e. this study: 1977-1994: -0.24 , -0.31 % year⁻¹ and 2009-2019: -0.41 , -0.63 % year⁻¹.

415 Unsurprisingly, the smaller glaciers are of greatest concern in relation to the implications for water resource provision,
416 given that they have shrunk the most over the past 42 years. Therefore, stress on water resources in the future is
417 expected to be greater, particularly around Leh Basin, where the majority of water resources derive from snow and
418 small glaciers melt only. The Leh Basin, situated between the Himalaya and Karakoram Ranges, displays a behaviour
419 more in line with the glaciers of Western Himalaya (Azam et al., 2018, 2021) and is significantly different from the
420 adjacent basins to the north (Shayok and Pangong) and to the south (Suru, Zaskar and Tsomoriri). Such a difference
421 is surprising yet understandable given the aridity and warmth of the climate in the valley (Figure 2, 8). This study
422 supports the findings by Chudley et al., 2017 and Schmidt & Nüsser, 2017 that the Leh Basin marks the transition
423 zone between the anomalous Karakoram, with its stable/surging glaciers, and the retreating Himalayan Range glaciers.

424

425 **6. Data availability**

426 For review purposes the data can be accessed via:
427 <https://www.pangaea.de/tok/8b9a6e7275b32019eab155e11a461866706fabf3> (Soheb et al., 2022).

428 The dataset will be available for public after the completion of the review process.

429 The entire dataset of the Landsat based multitemporal inventory of glaciers, larger than 0.5 km², in Ladakh
430 region for the year 1977, 1994, 2009 and 2019 will be available at:
431 PANGAEA, <https://doi.org/10.1594/PANGAEA.940994> (Soheb et al., 2022).

432



433 **7. Conclusions**

434 We compiled new glacier inventories of the UIB and IDBs within the Ladakh region for 1977, 1994, 2009 and 2019
435 using Landsat images. The inventory includes 2257 glaciers, larger than 0.5 km², covering an area of ~7923 ±212
436 km², which is ~14% and ~11% less than the RGI 6.0 and the GAMDAM, and 7% more than the ICIMOD inventories.
437 The glaciers range in area between 0.5 to 862 km², with most of them belonging to the smallest size category (0.5-1
438 km²) which account for ~694 km². The seven largest glaciers >100 km² account for the second largest glacierised area
439 of ~1879 km². Shayok Basin hosts the highest number of glaciers and glacierised area; whereas, Tsokar Basin has the
440 least. More than 70% of the glaciers are north-facing (NW-N-NE) and concentrated in higher elevation zones between
441 5000 and 6000 m a.s.l.

442 The study found that nearly all the glaciers (~97%) retreated and cumulatively lost a significant area of ~588 km² (-
443 6.9%) between 1977 and 2019. The retreat rates vary across the basins and glacier area categories. The relative area
444 loss was highest in Leh, Tsokar and Tsomoriri Basins and for the small glacier categories. In the Shayok Basin and
445 for the largest glaciers the relative area loss was lower. Smaller glaciers (0.5-1 and 1-5 km²) have retreated most with
446 a change of ~24 and ~11% (1977-2019). In other area categories, the retreat was less than 4%, with minimum change
447 (~-0.5%) found in the largest glacier area class of > 100 km². All basins showed a reduction in glacierised area of >10%
448 except Shayok Basin, where the change was just 3.9% due to more favourable climatic conditions and the presence of
449 surge-type and stable glaciers. The length change of individual glaciers was between +13 and -59% with a mean
450 change of -12% (-0.27% year⁻¹) over 42 years.

451 Meteorological records show a statistically significant increasing trend in mean annual temperature, with the highest
452 rate of +0.04 °C year⁻¹ observed in Leh. The annual precipitation trend was statistically significant only for Shiquanhe
453 (+0.74 mm year⁻¹) and Rutog (+0.93 mm year⁻¹). An increasing trend in JJAS and winter temperature was observed
454 for all locations, while an increasing trend in JJAS precipitation was found in Shiquanhe and Rutog only. Leh was the
455 warmest and driest basin, with annual PDDs and precipitation of >3000 °C and <120 mm, respectively. A statistically
456 significant positive trend in PDDs was observed for all the locations, and a decreasing trend in solid precipitation was
457 found in Shiquanhe and Tsomoriri.

458 The new multi-temporal inventory presented here will assist in planning the management of water resources, and for
459 guiding scientific research focusing on glacier mass balance, hydrology and glacier change within the region. The
460 detailed information and multi-temporal nature of this inventory will also aid in improving the existing global and
461 regional inventories especially in the cold-arid Ladakh region where the majority of the population is highly dependent
462 on glacier-derived melt water resources for domestic, irrigation and hydropower generation needs.

463

464 **Author contribution**

465 MSo, AR, AB conceptualized and designed the study. MSo, AB and MC did the analysis. MSo wrote and AR, AB,
466 MSp, BR, SS and LS edited the manuscript. All the authors have equally contributed to interpretation of the results.

467



468 **Acknowledgements**

469 The authors are thankful to the School of Environmental Sciences, Jawaharlal Nehru University, New Delhi, India,
470 for the lab facilities and the United States Geological Survey for the Landsat and ASTER imageries. The authors also
471 thank Planet Labs and Google for the high resolution PlanetScope and Google Earth imageries. We are also thankful
472 to the Scottish Funding Council and the University Of Aberdeen, United Kingdom for financially supporting our work.

473

474 **References**

475 Azam, M. F., Wagnon, P., Berthier, E., Vincent, C., Fujita, K., & Kargel, J. S. (2018). Review of the status and mass
476 changes of Himalayan-Karakoram glaciers. *Journal of Glaciology*, 64(243), 61–74.
477 <https://doi.org/10.1017/jog.2017.86>

478 Azam, Mohd. F., Kargel, J. S., Shea, J. M., Nepal, S., Haritashya, U. K., Srivastava, S., Maussion, F., Qazi, N.,
479 Chevallier, P., Dimri, A. P., Kulkarni, A. V., Cogley, J. G., & Bahuguna, I. M. (2021). Glaciohydrology of
480 the Himalaya-Karakoram. *Science*, eabf3668. <https://doi.org/10.1126/science.abf3668>

481 Bajracharya, S. R., Maharjan, S. B., & Shrestha, F. (2019). Glaciers in the Indus Basin. In *Indus River Basin* (pp. 123–
482 144). Elsevier. <https://doi.org/10.1016/B978-0-12-812782-7.00006-0>

483 Barrett, K., & Bosak, K. (2018). The Role of Place in Adapting to Climate Change: A Case Study from Ladakh,
484 Western Himalayas. *Sustainability*, 10(4), 898. <https://doi.org/10.3390/su10040898>

485 Bhambri, R., Bolch, T., Chaujar, R. K., & Kulshreshtha, S. C. (2011). Glacier changes in the Garhwal Himalaya,
486 India, from 1968 to 2006 based on remote sensing. *Journal of Glaciology*, 57(203), 543–556.
487 <https://doi.org/10.3189/002214311796905604>

488 Bhambri, R., Bolch, T., Kawishwar, P., Dobhal, D. P., Srivastava, D., & Pratap, B. (2013). Heterogeneity in glacier
489 response in the upper Shyok valley, northeast Karakoram. *The Cryosphere*, 7(5), 1385–1398.
490 <https://doi.org/10.5194/tc-7-1385-2013>

491 Bhambri, R., Hewitt, K., Kawishwar, P., & Pratap, B. (2017). Surge-type and surge-modified glaciers in the
492 Karakoram. *Scientific Reports*, 7(1), 15391. <https://doi.org/10.1038/s41598-017-15473-8>

493 Bhardwaj, A., Joshi, P., Snehamani, Sam, L., Singh, M. K., Singh, S., & Kumar, R. (2015). Applicability of Landsat 8
494 data for characterizing glacier facies and supraglacial debris. *International Journal of Applied Earth
495 Observation and Geoinformation*, 38, 51–64. <https://doi.org/10.1016/j.jag.2014.12.011>

496 Bolch, T. (2019). Past and Future Glacier Changes in the Indus River Basin. In *Indus River Basin* (pp. 85–97). Elsevier.
497 <https://doi.org/10.1016/B978-0-12-812782-7.00004-7>



- 498 Bolch, T., Kulkarni, A., Kaab, A., Huggel, C., Paul, F., Cogley, J. G., Frey, H., Kargel, J. S., Fujita, K., Scheel, M.,
499 Bajracharya, S., & Stoffel, M. (2012). The State and Fate of Himalayan Glaciers. *Science*, 336(6079), 310–
500 314. <https://doi.org/10.1126/science.1215828>
- 501 Bolch, T., Menounos, B., & Wheate, R. (2010). Landsat-based inventory of glaciers in western Canada, 1985–2005.
502 *Remote Sensing of Environment*, 114(1), 127–137. <https://doi.org/10.1016/j.rse.2009.08.015>
- 503 Chudley, T. R., Miles, E. S., & Willis, I. C. (2017). Glacier characteristics and retreat between 1991 and 2014 in the
504 Ladakh Range, Jammu and Kashmir. *Remote Sensing Letters*, 8(6), 518–527.
505 <https://doi.org/10.1080/2150704X.2017.1295480>
- 506 Farinotti, D., Immerzeel, W. W., de Kok, R. J., Quincey, D. J., & Dehecq, A. (2020). Manifestations and mechanisms
507 of the Karakoram glacier Anomaly. *Nature Geoscience*, 13(1), 8–16. <https://doi.org/10.1038/s41561-019-0513-5>
508
- 509 Frey, H., Machguth, H., Huss, M., Huggel, C., Bajracharya, S., Bolch, T., Kulkarni, A., Linsbauer, A., Salzmann, N.,
510 & Stoffel, M. (2014). Estimating the volume of glaciers in the Himalayan–Karakoram region
511 using different methods. *The Cryosphere*, 8(6), 2313–2333. <https://doi.org/10.5194/tc-8-2313-2014>
- 512 Granshaw, F. D., & G. Fountain, A. (2006). Glacier change (1958–1998) in the North Cascades National Park
513 Complex, Washington, USA. *Journal of Glaciology*, 52(177), 251–256.
514 <https://doi.org/10.3189/172756506781828782>
- 515 Guo, W., Liu, S., Xu, J., Wu, L., Shangguan, D., Yao, X., Wei, J., Bao, W., Yu, P., Liu, Q., & Jiang, Z. (2015). The
516 second Chinese glacier inventory: Data, methods and results. *Journal of Glaciology*, 61(226), 357–372.
517 <https://doi.org/10.3189/2015JoG14J209>
- 518 Hersbach, H., Bell, B., Berrisford, P., Hirahara, S., Horányi, A., Muñoz-Sabater, J., Nicolas, J., Peubey, C., Radu, R.,
519 Schepers, D., Simmons, A., Soci, C., Abdalla, S., Abellan, X., Balsamo, G., Bechtold, P., Biavati, G., Bidlot,
520 J., Bonavita, M., ... Thépaut, J. (2020). The ERA5 global reanalysis. *Quarterly Journal of the Royal
521 Meteorological Society*, 146(730), 1999–2049. <https://doi.org/10.1002/qj.3803>
- 522 Hewitt, K. (2005). The Karakoram Anomaly? Glacier Expansion and the ‘Elevation Effect,’ Karakoram Himalaya.
523 *Mountain Research and Development*, 25(4), 332–340. [https://doi.org/10.1659/0276-
524 4741\(2005\)025\[0332:TKAGEA\]2.0.CO;2](https://doi.org/10.1659/0276-4741(2005)025[0332:TKAGEA]2.0.CO;2)
- 525 Immerzeel, W. W., van Beek, L. P. H., & Bierkens, M. F. P. (2010). Climate Change Will Affect the Asian Water
526 Towers. *Science*, 328(5984), 1382–1385. <https://doi.org/10.1126/science.1183188>



- 527 Ines, A. V. M., & Hansen, J. W. (2006). Bias correction of daily GCM rainfall for crop simulation studies. *Agricultural*
528 *and Forest Meteorology*, 10.
- 529 Ji, Q., Yang, T., He, Y., Qin, Y., Dong, J., & Hu, F. (2017). A simple method to extract glacier length based on Digital
530 Elevation Model and glacier boundaries for simple basin type glacier. *Journal of Mountain Science*, 14(9),
531 1776–1790. <https://doi.org/10.1007/s11629-016-4243-5>
- 532 Käab, A., Treichler, D., Nuth, C., & Berthier, E. (2015). Brief Communication: Contending estimates of
533 2003–2008 glacier mass balance over the Pamir–Karakoram–Himalaya. *The Cryosphere*, 9(2),
534 557–564. <https://doi.org/10.5194/tc-9-557-2015>
- 535 Kanda, N., Negi, H. S., Rishi, M. S., & Kumar, A. (2020). Performance of various gridded temperature and
536 precipitation datasets over Northwest Himalayan Region. *Environmental Research Communications*, 2(8),
537 085002. <https://doi.org/10.1088/2515-7620/ab9991>
- 538 Khan, A., Richards, K. S., Parker, G. T., McRobie, A., & Mukhopadhyay, B. (2014). How large is the Upper Indus
539 Basin? The pitfalls of auto-delineation using DEMs. *Journal of Hydrology*, 509, 442–453.
540 <https://doi.org/10.1016/j.jhydrol.2013.11.028>
- 541 Kulkarni, A. V. (2010). *Monitoring Himalayan cryosphere using remote sensing techniques*. 90, 13.
- 542 Liu, S., Ding, Y., Shangguan, D., Zhang, Y., Li, J., Han, H., Wang, J., & Xie, C. (2006). Glacier retreat as a result of
543 climate warming and increased precipitation in the Tarim river basin, northwest China. *Annals of Glaciology*,
544 43, 91–96. <https://doi.org/10.3189/172756406781812168>
- 545 Maurer, J. M., Schaefer, J. M., Rupper, S., & Corley, A. (2019). Acceleration of ice loss across the Himalayas over
546 the past 40 years. *Science Advances*, 5(6), eaav7266. <https://doi.org/10.1126/sciadv.aav7266>
- 547 Minora, U., Bocchiola, D., D’Agata, C., Maragno, D., Mayer, C., Lambrecht, A., Mosconi, B., Vuillermoz, E., Senese,
548 A., Compostella, C., Smiraglia, C., & Diolaiuti, G. (2013). *2001–2010 glacier changes in the Central*
549 *Karakoram National Park: A contribution to evaluate the magnitude and rate of the “Karakoram*
550 *anomaly”*; [Preprint]. *Glaciers*. <https://doi.org/10.5194/tcd-7-2891-2013>
- 551 Minora, U., Bocchiola, D., D’Agata, C., Maragno, D., Mayer, C., Lambrecht, A., Vuillermoz, E., Senese, A.,
552 Compostella, C., Smiraglia, C., & Diolaiuti, G. A. (2016). Glacier area stability in the Central Karakoram
553 National Park (Pakistan) in 2001–2010: The “Karakoram Anomaly” in the spotlight. *Progress in Physical*
554 *Geography: Earth and Environment*, 40(5), 629–660. <https://doi.org/10.1177/0309133316643926>



- 555 Mölg, N., Bolch, T., Rastner, P., Strozzi, T., & Paul, F. (2018). A consistent glacier inventory for Karakoram and
556 Pamir derived from Landsat data: Distribution of debris cover and mapping challenges. *Earth System Science*
557 *Data*, 10(4), 1807–1827. <https://doi.org/10.5194/essd-10-1807-2018>
- 558 Müller, J., Dame, J., & Nüsser, M. (2020). Urban Mountain Waterscapes: The Transformation of Hydro-Social
559 Relations in the Trans-Himalayan Town Leh, Ladakh, India. *Water*, 12(6), 1698.
560 <https://doi.org/10.3390/w12061698>
- 561 Nagai, H., Fujita, K., Sakai, A., Nuimura, T., & Tadono, T. (2016). Comparison of multiple glacier inventories with
562 a new inventory derived from high-resolution ALOS imagery in the Bhutan Himalaya. *The Cryosphere*,
563 10(1), 65–85. <https://doi.org/10.5194/tc-10-65-2016>
- 564 Negi, H. S., Kumar, A., Kanda, N., Thakur, N. K., & Singh, K. K. (2021). Status of glaciers and climate change of
565 East Karakoram in early twenty-first century. *Science of The Total Environment*, 753, 141914.
566 <https://doi.org/10.1016/j.scitotenv.2020.141914>
- 567 Nüsser, M., Dame, J., Kraus, B., Baghel, R., & Schmidt, S. (2019). Socio-hydrology of “artificial glaciers” in Ladakh,
568 India: Assessing adaptive strategies in a changing cryosphere. *Regional Environmental Change*, 19(5), 1327–
569 1337. <https://doi.org/10.1007/s10113-018-1372-0>
- 570 Nüsser, M., Dame, J., Parveen, S., Kraus, B., Baghel, R., & Schmidt, S. (2019). Cryosphere-Fed Irrigation Networks
571 in the Northwestern Himalaya: Precarious Livelihoods and Adaptation Strategies Under the Impact of
572 Climate Change. *Mountain Research and Development*, 39(2). <https://doi.org/10.1659/MRD-JOURNAL-D-18-00072.1>
- 574 Paul, F., Barry, R. G., Cogley, J. G., Frey, H., Haerberli, W., Ohmura, A., Ommanney, C. S. L., Raup, B., Rivera, A.,
575 & Zemp, M. (2009). Recommendations for the compilation of glacier inventory data from digital sources.
576 *Annals of Glaciology*, 50(53), 119–126. <https://doi.org/10.3189/172756410790595778>
- 577 Paul, F., Bolch, T., Briggs, K., Kääb, A., McMillan, M., McNabb, R., Nagler, T., Nuth, C., Rastner, P., Strozzi, T., &
578 Wuite, J. (2017). Error sources and guidelines for quality assessment of glacier area, elevation change, and
579 velocity products derived from satellite data in the Glaciers_cci project. *Remote Sensing of Environment*,
580 203, 256–275. <https://doi.org/10.1016/j.rse.2017.08.038>
- 581 Pfeffer, W. T., Arendt, A. A., Bliss, A., Bolch, T., Cogley, J. G., Gardner, A. S., Hagen, J.-O., Hock, R., Kaser, G.,
582 Kienholz, C., Miles, E. S., Moholdt, G., Mölg, N., Paul, F., Radić, V., Rastner, P., Raup, B. H., Rich, J.,
583 Sharp, M. J., & The Randolph Consortium. (2014). The Randolph Glacier Inventory: A globally complete
584 inventory of glaciers. *Journal of Glaciology*, 60(221), 537–552. <https://doi.org/10.3189/2014JG13J176>



- 585 Pritchard, H. D. (2019). Asia's shrinking glaciers protect large populations from drought stress. *Nature*, 569(7758),
586 649–654. <https://doi.org/10.1038/s41586-019-1240-1>
- 587 Racoviteanu, A. E., Paul, F., Raup, B., Khalsa, S. J. S., & Armstrong, R. (2009). Challenges and recommendations in
588 mapping of glacier parameters from space: Results of the 2008 Global Land Ice Measurements from Space
589 (GLIMS) workshop, Boulder, Colorado, USA. *Annals of Glaciology*, 50(53), 53–69.
590 <https://doi.org/10.3189/172756410790595804>
- 591 Sakai, A. (2019). Brief communication: Updated GAMDAM glacier inventory over high-mountain Asia. *The*
592 *Cryosphere*, 13(7), 2043–2049. <https://doi.org/10.5194/tc-13-2043-2019>
- 593 Schmidt, S., & Nüsser, M. (2012). Changes of High Altitude Glaciers from 1969 to 2010 in the Trans-Himalayan
594 Kang Yatze Massif, Ladakh, Northwest India. *Arctic, Antarctic, and Alpine Research*, 44(1), 107–121.
595 <https://doi.org/10.1657/1938-4246-44.1.107>
- 596 Schmidt, S., & Nüsser, M. (2017). Changes of High Altitude Glaciers in the Trans-Himalaya of Ladakh over the Past
597 Five Decades (1969–2016). *Geosciences*, 7(2), 27. <https://doi.org/10.3390/geosciences7020027>
- 598 Sen, P. K. (1968). Estimates of the Regression Coefficient Based on Kendall's Tau. *Journal of the American Statistical*
599 *Association*, 63(324), 1379–1389. <https://doi.org/10.1080/01621459.1968.10480934>
- 600 Shean, D. E., Bhushan, S., Montesano, P., Rounce, D. R., Arendt, A., & Osmanoglu, B. (2020). A Systematic,
601 Regional Assessment of High Mountain Asia Glacier Mass Balance. *Frontiers in Earth Science*, 7, 363.
602 <https://doi.org/10.3389/feart.2019.00363>
- 603 Shrestha, M., Acharya, S. C., & Shrestha, P. K. (2017). Bias correction of climate models for hydrological
604 modelling – are simple methods still useful? *Meteorol. Appl.*, 9.
- 605 Shukla, A., Garg, S., Mehta, M., Kumar, V., & Shukla, U. K. (2020). Temporal inventory of glaciers in the Suru sub-
606 basin, western Himalaya: Impacts of regional climate variability. *Earth System Science Data*, 12(2), 1245–
607 1265. <https://doi.org/10.5194/essd-12-1245-2020>
- 608 Singh, S., Kumar, R., Bhardwaj, A., Sam, L., Shekhar, M., Singh, A., Kumar, R., & Gupta, A. (2016). Changing
609 climate and glacio-hydrology in Indian Himalayan Region: A review. *WIREs Climate Change*, 7(3), 393–
610 410. <https://doi.org/10.1002/wcc.393>
- 611 Soheb, M., Ramanathan, A., Angchuk, T., Mandal, A., Kumar, N., & Lotus, S. (2020). Mass-balance observation,
612 reconstruction and sensitivity of Stok glacier, Ladakh region, India, between 1978 and 2019. *Journal of*
613 *Glaciology*, 66(258), 627–642. <https://doi.org/10.1017/jog.2020.34>



- 614 Soheb, Mohd; Ramanathan, Alagappan; Bhardwaj, Anshuman; Coleman, Millie; Rea, Brice; Spagnolo,
615 Matteo; Singh, Shaktiman; Sam, Lydia (2022): Landsat based multitemporal glacier inventory data of over
616 four decades (1977-2019) in Ladakh region. *PANGAEA*, <https://doi.org/10.1594/PANGAEA.940994>
- 617 Teutschbein, C., & Seibert, J. (2013). Is bias correction of regional climate model (RCM) simulations possible for
618 non-stationary conditions? *Hydrology and Earth System Sciences*, 17(12), 5061–5077.
619 <https://doi.org/10.5194/hess-17-5061-2013>
- 620 Tielidze, L. G., & Wheate, R. D. (2018). The Greater Caucasus Glacier Inventory (Russia, Georgia and Azerbaijan).
621 *The Cryosphere*, 12(1), 81–94. <https://doi.org/10.5194/tc-12-81-2018>
- 622 Williams, M. W. (2013). The Status of Glaciers in the Hindu Kush–Himalayan Region. *Mountain Research and*
623 *Development*, 33(1), 114. <https://doi.org/10.1659/mrd.mm113>
- 624 Winsvold, S. H., Kaab, A., & Nuth, C. (2016). Regional Glacier Mapping Using Optical Satellite Data Time Series.
625 *IEEE Journal of Selected Topics in Applied Earth Observations and Remote Sensing*, 9(8), 3698–3711.
626 <https://doi.org/10.1109/JSTARS.2016.2527063>
- 627 Yang, R., Hock, R., Kang, S., Shangguan, D., & Guo, W. (2020). Glacier mass and area changes on the Kenai
628 Peninsula, Alaska, 1986–2016. *Journal of Glaciology*, 66(258), 603–617.
629 <https://doi.org/10.1017/jog.2020.32>
- 630 Yao, T., Thompson, L., Yang, W., Yu, W., Gao, Y., Guo, X., Yang, X., Duan, K., Zhao, H., Xu, B., Pu, J., Lu, A.,
631 Xiang, Y., Kattel, D. B., & Joswiak, D. (2012). Different glacier status with atmospheric circulations in
632 Tibetan Plateau and surroundings. *Nature Climate Change*, 2(9), 663–667.
633 <https://doi.org/10.1038/nclimate1580>
- 634 Zhang, M., Wang, X., Shi, C., & Yan, D. (2019). Automated Glacier Extraction Index by Optimization of Red/SWIR
635 and NIR /SWIR Ratio Index for Glacier Mapping Using Landsat Imagery. *Water*, 11(6), 1223.
636 <https://doi.org/10.3390/w11061223>
- 637